In-Situ FTIR Study of Adsorption and Photoreactions of CH_2Cl_2 on Powdered TiO_2

Meng-Tso Chen, Chen-Fu Lien, Li-Fen Liao, and Jong-Liang Lin*

Department of Chemistry, National Cheng Kung University, Tainan, Taiwan, Republic of China

Received: September 18, 2002; In Final Form: December 31, 2002

The adsorption and photoreactions of CH_2Cl_2 on powdered TiO_2 have been investigated by Fourier transform infrared spectroscopy. CH_2Cl_2 is adsorbed molecularly or dissociatively to form chloromethoxy ($CClH_2O_{(a)}$) at 35 °C. $CClH_2O_{(a)}$ decomposes into $CH_3O_{(a)}$ and $HCOO_{(a)}$ in a vacuum at temperatures higher than ∼100 °C. As TiO_2 in contact with gaseous CH_2Cl_2 is heated in a closed cell, HCl from $Cl_{(a)}$ and $OH_{(a)}$ recombination, CH_2O from $CH_3O_{(a)}$ decomposition, and CO and CO_2 from $HCOO_{(a)}$ decomposition are detected. In the $CH_2Cl_{2(a)}$ photodecomposition in the absence of O_2, $CO_{(a)}$, $CO_{3(a)}$, and $HCOO_{(a)}$ are generated. The TiO_2-mediated $CH_2Cl_{2(a)}$ photodecomposition is likely initiated by surface-active oxygen species instead of direct hole transfer. In the presence of O_2, $CH_2Cl_{2(a)}$ photodecomposition is accelerated. In addition to $CO_{(a)}$, $CO_{3(a)}$, and $HCOO_{(a)}$, $H_2O_{(a)}$ and $CO_{2(a)}$ are generated as well. In the case of $CO_{(a)}$ formation, O_2 is also involved in addition to TiO_2 lattice oxygen. The O_2 participation may be via oxygen anion species.

Introduction

Halogenated hydrocarbons have been widely employed as chemical reagents and solvents. Their presence in underground water and in the atmosphere has caused profound impact on the ozone layer depletion and human health. A promising approach involving photocatalysis of a semiconductor to degrade environmentally hazardous chemicals has been developed recently.[1] It utilizes the reductive and oxidative ability of electron−hole pairs as the band-gap of a semiconductor is excited with photons. TiO_2 is often used for this purpose because it is economically inexpensive, chemically stable, and its band-gap excitation energy overlaps with the solar spectrum.

Methylene halides are an important subgroup of halogenated hydrocarbons used in the laboratory and in industry. TiO_2 photocatalytically assisted degradation of CH_2Cl_2 has been investigated.[2−5] Calza et al. showed that in the presence of O_2, CH_2Cl_2 was almost converted to CO_2 and Cl^- in an aqueous solution of pH = 5, with reaction intermediates of CH_3OH, H_2CO, and HCOOH detected by chromatography.[2] They also studied the photodecomposition rate of CH_2Cl_2 in the absence or presence of O_2 and the effect of scavenger of electron or hole.[3] Lichtin et al. investigated the decomposition of CH_2Cl_2 vapor over TiO_2 in the presence of O_2 and found the formation of $COCl_2$, CO, and Cl_2.[4] However, in these previous studies, adsorption and surface reactions were not characterized. In the present research, we apply Fourier transform infrared spectroscopy to study the adsorption and thermal reactions and photochemistry of CH_2Cl_2 on TiO_2. Study of the interaction of CH_2Cl_2 vapor with TiO_2 is interesting and important from the standpoint of atmosphere cleaning. In addition, it may also provide direct, in-situ monitoring of the reaction process and help to further elucidate the mechanism for reactions in solution phase.

Experimental Section

The sample preparation of TiO_2 powder supported on a tungsten fine mesh (∼6 cm^2) has been described previously.[6,7] In brief, TiO_2 powder (Degussa P25, ∼50 m^2/g, anatase 70%, rutile 30%) was dispersed in water/acetone solution to form a uniform mixture which was then sprayed onto a tungsten mesh. After that, the TiO_2 sample was mounted inside the IR cell for simultaneous photochemistry and FTIR spectroscopy. The IR cell with two CaF_2 windows for IR transmission down to 1000 cm^{-1} was connected to a gas manifold which was pumped by a 60 L/s turbomolecular pump with a base pressure of ∼1×10^{-7} Torr. The TiO_2 sample in the cell was heated to 450 °C under vacuum for 24 h by resistive heating. The temperature of TiO_2 sample was measured by a K-type thermocouple spot-welded on the tungsten mesh. Before each run of the experiment, the TiO_2 sample was heated to 450 °C in a vacuum for 2 h. After the heating, 10 Torr of O_2 was introduced into the cell as the sample was cooled to 70 °C. When the TiO_2 temperature reached 35 °C, the cell was evacuated for gas dosing. The TiO_2 surface after the above treatment still possessed residual isolated hydroxyl groups. O_2 (99.998%, Matheson), and $^{18}O_2$ (99 at. %, Isotec) were used as received in compressed states. CH_2Cl_2 (99.5%, Merck) was purified by several cycles of freeze−pump−thaw prior to introduction to the cell. Pressure was monitored with a Baratron capacitance manometer and an ion gauge. In the photochemistry study, both the UV and IR beams were set 45° to the normal of the TiO_2 sample. The UV light source used was a combination of a Hg arc lamp (Oriel Corp), a water filter, and a band-pass filter with a bandwidth of ∼100 nm centered at ∼400 nm (Oriel 51670). The UV absorption of CH_2Cl_2 for the wavelength used in the present study was negligible.[8] Infrared spectra were obtained with a 4 cm^{-1} resolution by a Bruker FTIR spectrometer with a MCT detector. The entire optical path was purged with CO_2-free dry air. The spectra presented here have been ratioed against a clean TiO_2 spectrum providing the metal-oxide background. In the study of photo-oxidation, the photoirradiation time count was started as the UV lamp was turned on. It took 40−50 s to reach full power.

Results and Discussion

Adsorption and Thermal Transformation of Adsorbed CH_2Cl_2 on TiO_2. Figure 1 shows the IR spectra of TiO_2 after being in contact with 2 Torr of CH_2Cl_2 vapor at 35 °C followed

* Corresponding author. Phone: 886 6 2757575, ext. 65326. Fax: 886 6 2740552. E-mail: jonglin@mail.ncku.edu.tw.

10.1021/jp0220884 CCC: $25.00
Published on Web 03/29/2003

TABLE 1: Vibrational Frequencies (cm^{-1}) and Mode Assignments for CH_2Cl_2 Adsorbed on TiO_2 at 35 and 200 °C

on TiO_2 35 °C	on TiO_2 200 °C	$CH_2Cl_{2(g)}$ (ref 9)	CH_2Cl_2/Pd/SiO_2 at −60 °C (ref 10)	approximate mode of CH_2Cl_2	$HCOO/TiO_2$ (ref 11)	approximate mode of HCOO(a)	CH_3O/TiO_2 (refs 11,12)	approximate mode of $CH_3O_{(a)}$
1116								
1151	1151						1045, 1126	ν(C−O)
1261		1261, 1268, 1275		$\omega(CH_2)$				
	1363				1359	ν_s(COO)		
	1381				1386	δ(CH)		
1417		1462, 1473	1426	$\delta(CH_2)$				
	1552				1552	ν_{as}(COO)		
	2775				2754	ν_s(COO) + δ(CH)		
	2836						2828	$\nu_s(CH_3)$
2881	2881							
	2890				2872	ν(CH)		
	2936						2929	$\nu_{as}(CH_3)$
	2960				2952	ν_{as}(COO) + δ(CH)		
2989		2991, 3007	2984	$\nu_s(CH_2)$				
3060		3045(liquid)	3064	$\nu_{as}(CH_2)$				

by evacuation at 35, 50, 100, 150, 200, and 250 °C for 1 min. In the 35 °C spectrum, absorption peaks appear at 1116, 1151, 1261, 1417, 2881, 2989, and 3060 cm^{-1}. As the temperature is increased to 50 °C, the peak intensities of 1261, 1417, 2989, and 3060 cm^{-1} are simultaneously reduced by the same proportion of ∼50%, suggesting that these four bands result from a same surface species. In terms of the similar frequencies of CH_2Cl_2 observed in gas phase[9] and on Pd-loaded SiO_2[10] surface as shown in Table 1, these four bands are attributed to CH_2Cl_2 adsorbed molecularly on TiO_2. The 1261, 1417, 2989, and 3060 cm^{-1} are assigned to CH_2 wagging, scissoring, symmetric stretching, and antisymmetric stretching, respectively. The amount of the surface CH_2Cl_2 decreases with increasing temperature. The disappearance of the most intense 3060 cm^{-1} peak of adsorbed CH_2Cl_2 in Figure 1 shows that it is completely removed above 150 °C. The other bands of 1116, 1151, and 2881 cm^{-1} observed in the 35 °C spectrum do not belong to adsorbed CH_2Cl_2 and show thermal behavior different from that of $CH_2Cl_{2(a)}$. The 2881 cm^{-1} intensity reaches a maximum between 100 and 150 °C and diminishes gradually above ∼150 °C. The species responsible for the three bands is discussed latter. In Figure 1, absorptions at 1151, 1363, 1381, 1552, 2775, 2836, 2890, 2936, and 2960 cm^{-1} develop as the temperature is increased above ∼100 °C. Among them, the three bands at 1151, 2836, and 2936 cm^{-1} are similar to the previous FTIR studies of dissociative adsorption of CH_3OH on TiO_2 and are assigned to C−O stretching and CH_3 symmetric and antisymmetric stretching of adsorbed $CH_3O_{(a)}$ groups, respectively.[11,12] The other bands at 1363, 1381, 1552, 2775, 2890, and 2960 cm^{-1} are similar to the IR frequencies of dissociative formic acid adsorption on TiO_2 and therefore are attributed to adsorbed formate.[11] Table 1 lists the previously observed frequencies of $CH_3O_{(a)}$ and $HCOO_{(a)}$ on TiO_2 and their corresponding vibrational modes for comparison. Close inspection of the spectral changes between 150 and 250 °C shows that $CH_3O_{(a)}$ and $HCOO_{(a)}$ appear at the expense of the species responsible for the 2881 cm^{-1} band, because in this temperature range the 2881 cm^{-1} intensity is decreased in contrast to the development of the $CH_3O_{(a)}$ and $HCOO_{(a)}$ bands. Note that $CH_3O_{(a)}$ and $HCOO_{(a)}$ formation is not due to direct $CH_2Cl_{2(a)}$ dissociation. The most intense $CH_2Cl_{2(a)}$ peak of 3061 cm^{-1} is only barely visible at 150 °C and completely disappears at 200 °C, showing that no more CH_2Cl_2 is present on the surface at this temperature. However, as the temperature is increased from 200 °C to 250 °C, $CH_3O_{(a)}$ and $HCOO_{(a)}$ are increased by ∼10% and ∼45%, respectively, estimated by the increase of their characteristic peaks at 2836 and 1363 cm^{-1}.

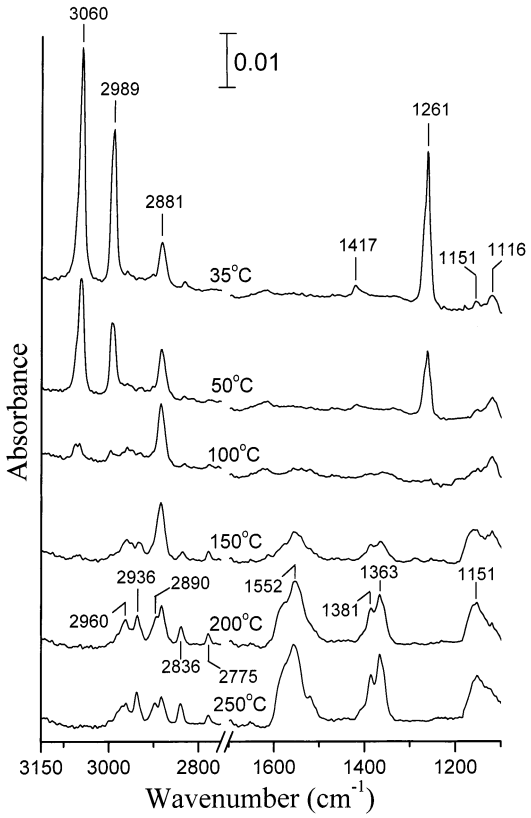

Figure 1. Infrared spectra of TiO_2 in contact with 2 Torr of CH_2Cl_2 at 35 °C followed by evacuation at 35, 50, 100, 150, 200, and 250 °C for 1 min. All of the spectra were measured at 35 °C with 50 scans.

We now discuss the possible species that are responsible for the bands of 1116, 1151, and 2881 cm^{-1}. The 2881 cm^{-1} is a characteristic frequency of CH_x stretching, and 1116 and 1151 cm^{-1} are likely due to C−O stretching. The possible surface species with these bonding features from C−Cl or C−H bond breakage of CH_2Cl_2 are included in Scheme 1. It is assumed that the molecular fragments after the C−Cl or C−H bond scission of CH_2Cl_2 are bonded to the surface oxygen of TiO_2, because it is found that, in the case of dissociation of CH_3I on TiO_2, $CH_3O_{(a)}$ is generated after C−I bond breakage.[13] To find out the most probable structure for the 1116, 1151, and 2881 cm^{-1} bands, the thermal reaction result needs to be taken into account, i.e., as this structure decomposes, it generates $CH_3O_{(a)}$ and $HCOO_{(a)}$ simultaneously. Previously, Busca et al. studied

SCHEME 1

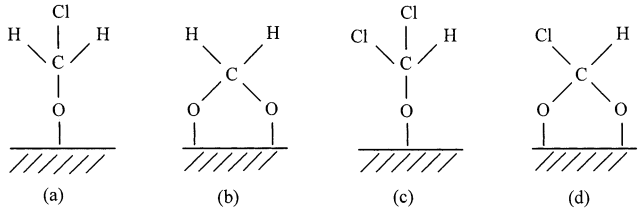

SCHEME 2

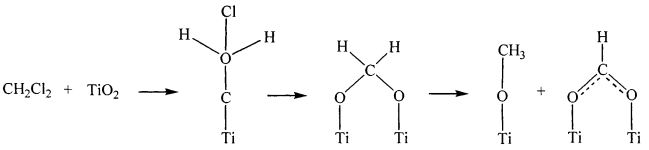

the adsorption and thermal reactions of CH_2O on TiO_2 by FTIR.[14] They observed the formation of dioxymethylene (Scheme 1b) resulting from the interaction between CH_2O and the surface below 30 °C. The dioxymethylene completely decomposes via oxidation to form $HCOO_{(a)}$ and via Cannizzaro-type disproportionation to form $HCOO_{(a)}$ and $CH_3O_{(a)}$ simultaneously prior to 150 °C. Although the species with the 1116, 1151, and 2881 cm^{-1} bands in Figure 1 has similar thermal reaction products of $HCOO_{(a)}$ and $CH_3O_{(a)}$, Scheme 1b is not the species responsible for the three bands, because they are still observable in Figure 1 at 150 °C, the temperature dioxymethylene is not stable on the surface. But it is very likely that dioxymethylene is the transient reaction intermediate that originated from the thermal decomposition of the species with the bands at 1116, 1151, 2881 cm^{-1} at temperatures higher than 100 °C. If this is true, it suggests that the structure of Scheme 1a, which can lose the Cl atom to form dioxymethylene, is responsible the three bands. From the point of view of bond strength, it also supports that Scheme 1a is generated from CH_2Cl_2 decomposition, because the bond energy of C−Cl (∼355 kJ/mol) is lower than that of C−H bond (∼420 kJ/mol) and may be broken more easily. Part c and d in Scheme 1 possess only one C−H bond, their hydrogenation to form $CH_3O_{(a)}$ in a vacuum has not been reported and is unlikely to occur. Scheme 2 summarizes the proposed thermal reaction pathway for adsorbed CH_2Cl_2 on TiO_2. Figure 1 shows chemical reactions that only involve surface species. Because these results were obtained as the surface was heated under vacuum, it was unlikely that the reaction products of $CH_3O_{(a)}$ and $HCOO_{(a)}$ were due to readsorption of gaseous products.

Figure 2 is the development of infrared spectra of 30 Torr of CH_2Cl_2 over a TiO_2 surface heated at a rate of 2 °C/s and then cooled in a closed cell to show gaseous products from CH_2Cl_2 thermal decomposition. Only several representative spectra are exhibited. All of the spectra in Figure 2 were taken at the indicated temperatures during the surface heating and cooling processes. In the 35 °C spectrum before heating, the major peaks from contribution of adsorbed and gaseous CH_2Cl_2 appear at 1261, 1274, 2989, 3005, and 3059 cm^{-1}, corresponding to CH_2 wagging and stretching modes,[9] with several small bands due to combination modes. As the temperature is increased to 100 °C, the band at 3059 cm^{-1} is largely reduced, showing that adsorbed CH_2Cl_2 is subject to desorption at higher temperatures. Above ∼130 °C, $CH_3O_{(a)}$ represented by 2839 and 2945 cm^{-1} and $HCOO_{(a)}$ represented by 1357 and 1544 cm^{-1} are generated, as seen in the 200 °C spectrum. On further heating to ∼300 °C, adsorbed CH_2Cl_2 represented by 3059 cm^{-1} is no longer observed. Above ∼315 °C, $CH_3O_{(a)}$ and $HCOO_{(a)}$ almost

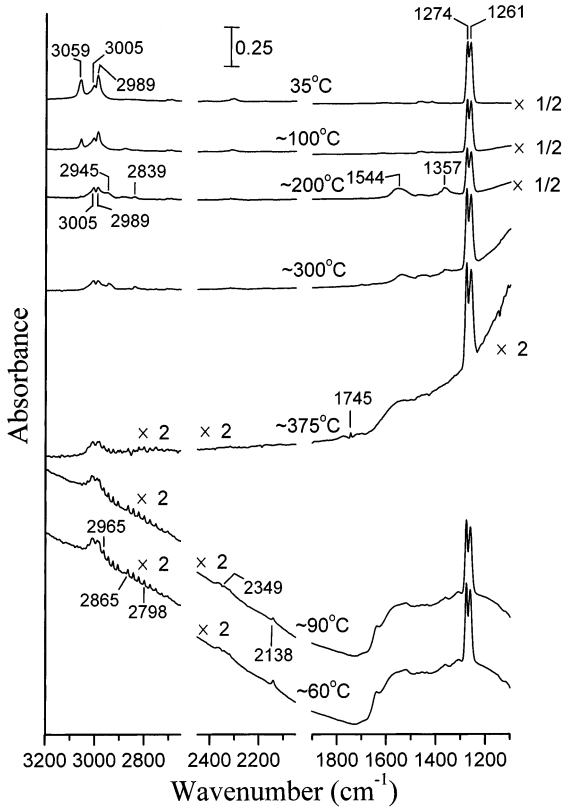

Figure 2. Infrared spectra obtained at the indicated temperatures during the heating from 35 °C to 400 °C at the rate of 2 °C/s for a TiO_2 surface initially in contact with 30 Torr of CH_2Cl_2, followed by holding the surface temperature at 400 °C for 3 min and then cooling. All of the spectra were measured with 5 scans.

disappear and new bands appear at 1745 cm^{-1} and in the region of 2700−3050 cm^{-1} together with the original gaseous CH_2Cl_2 absorptions at 1261, 1274, 2989, and 3005 cm^{-1}. The 1745 cm^{-1} band position and shape indicate the formation of CH_2O in the gas phase.[15] After heating the surface to 400 °C for 3 min and then cooling, the spectra at 90 and 60 °C show that the $CH_2O_{(g)}$ peak becomes barely visible while the bunch of the bands scattered between 2700 and 3050 cm^{-1} becomes clearer. The representative peak positions at 2798, 2865, and 2965 cm^{-1} stand for the formation of gaseous HCl.[15] In addition, the bands at 2138 and 2349 $cm^{-1}$are attributed to adsorbed CO and gaseous CO_2, respectively. Previous studies have shown that CH_2O is a thermal decomposition product of $CH_3O_{(a)}$ and that CO and CO_2 can be produced from $HCOO_{(a)}$.[11] In Figure 2, after increasing the temperature to 400 °C, there is a strong, broad absorption feature as shown in the 1100−1900 cm^{-1} region of the 90 and 60 °C spectra. Although detailed assignments for the responsible species are impossible, they are likely due to formate, methoxy, carbonyl-containing species and/or polymer chains from CH_2O condensation.[14]

Photooxidation of Adsorbed CH_2Cl_2. Figure 3 shows the infrared spectra taken before and after the indicated times during UV exposure of CH_2Cl_2 on the TiO_2 surface in a closed cell. It is found that the $CH_2Cl_{2(a)}$ is gradually decreased with UV irradiation as demonstrated by the gradual reduction of the peaks at 1261, 2989, and 3060 cm^{-1}. After 180 min, ∼85% of adsorbed CH_2Cl_2 has disappeared to enhance the absorptions at 1326, 1357, 1448, 1571, 2129, and 2956 cm^{-1}. The appearaance of 2129 cm^{-1} suggests the formation of adsorbed CO, because gaseous CO absorbs at 2143 cm^{-1}.[15] To further confirm this assignment, we carried out a CO adsorption experiment and present the result in Figure 4a. In this spectrum,

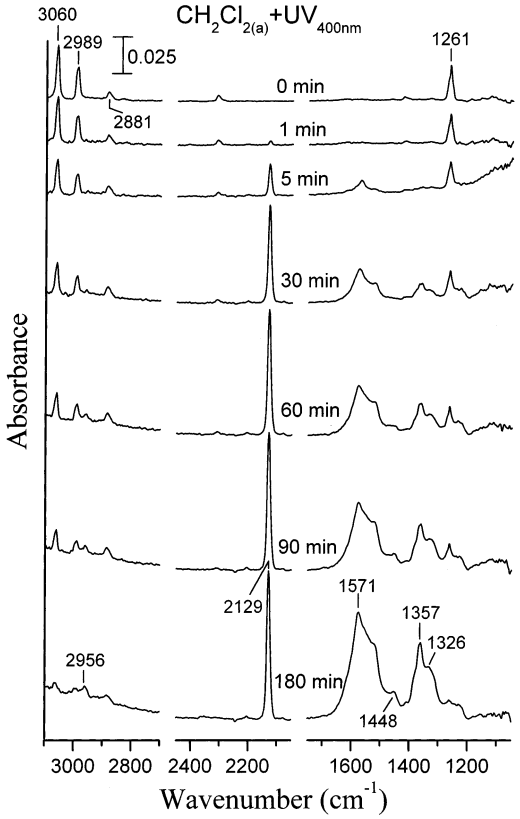

Figure 3. Infrared spectra taken after the indicated times during photoirradation of a TiO_2 surface covered with CH_2Cl_2. The CH_2Cl_2-adsorbed surface was prepared by exposing a clean TiO_2 surface to 2 Torr of CH_2Cl_2 followed by evacuation at 35 °C. All of the spectra were measured with 5 scans.

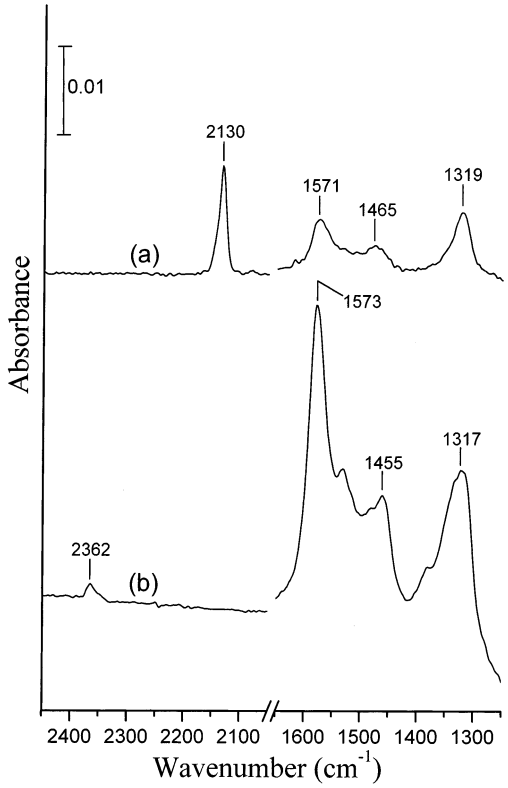

Figure 4. Infrared spectrum of TiO_2 after being in contact with 3 Torr of CO followed by evacuation at 35 °C (a); infrared spectrum of TiO_2 after being in contact with 0.1 Torr of CO_2 followed by evacuation at 35 °C (b).

there are four bands at 1319, 1465, 1571, and 2130 cm^{-1} after CO adsorption on TiO_2, which match those at 1326, 1448, 1571, and 2129 cm^{-1} in Figure 3. In addition to the $CO_{(a)}$ formation (2129 cm^{-1}), the 1326, 1448, and 1571 cm^{-1} are attributed to adsorbed carbonate which has been identified by FTIR studies of CO_2 adsorption on various metal oxides.[16−24] Specifically, the 1326 and 1571 cm^{-1} are due to bidentate carbonate, and 1448 cm^{-1} is due to monodentate or free carbonate. Besides, the bands at 1357, 1571, and 2956 cm^{-1} indicate that formate is generated as well. These products increase monotonically at the sacrifice of $CH_2Cl_{2(a)}$ due to photodecomposition. In Figure 3, the 2881 cm^{-1} band from $CClH_2O_{(a)}$ is present on the surface almost without changing its intensity during the photoirradiation.

Figure 5 shows the infrared spectra taken before and after the indicated times during UV exposure of CH_2Cl_2 adsorbed on TiO_2 surface in 10 Torr of O_2. The $CH_2Cl_{2(a)}$ are hardly detectable after 60 min UV irradiation that is much faster than the case without oxygen. The bands at 1319, 1353, 1457, 1569, and 2127 cm^{-1} develop along with the light exposure, indicating the formation of carbonate, formate, and CO. Two other new bands, which are not found in the absence of O_2, appear at 1615 and 2353 cm^{-1}. The 1615 cm^{-1} is attributed to adsorbed water. The 2353 cm^{-1} band suggests the formation of adsorbed CO_2. The $CO_{2(a)}$ assignment is further confirmed by CO_2 adsorption on TiO_2 as shown in the spectrum of Figure 4b. The bands observed in Figure 4b are attributed to adsorbed CO_2 (2362 cm^{-1}) and carbonate (1317, 1455, and 1573 cm^{-1}). In the presence of O_2, $CO_{(a)}$ is no more increased continuously. It reaches a maximum amount at ∼10 min and then declines. The $CO_{2(a)}$ formation is apparently due to photooxidation of adsorbed CO in the presence of O_2. Another pathway to form $CO_{2(a)}$ is the photodecomposition of formate which has been demonstrated previously.[25] Unlike the case without O_2, $CClH_2O_{(a)}$ at 2881 cm^{-1} is completely consumed after ∼60 min irradiation. Detailed variations of the amounts of adsorbed CH_2Cl_2, CO, and CO_2 with UV irradiation time in the presence and absence of O_2 are shown in Figure 6. For both cases, the amounts of initial surface CH_2Cl_2 are the same. The CH_2Cl_2 peaks are no longer observed at ∼80 min photoillumination in O_2, while 40% of the initial CH_2Cl_2 is still present on the surface without O_2. TiO_2-catalyzed CH_2Cl_2 photodecomposition is accelerated by O_2, because the CH_2Cl_2 decreasing rate is larger in Figure 6. Note that, since the surface temperature is increased to ∼50 °C during the UV illumination, the consumption of adsorbed CH_2Cl_2 is in part due to desorption as supported by the result of Figure 1.

In the photodecomposition of $CH_2Cl_{2(a)}$ in the absence of O_2, TiO_2 lattice oxygen anions must be involved in order to form $CO_{(a)}$. Therefore there is an intriguing question about the role of O_2 in the formation of $CO_{(a)}$ during photodecomposition of CH_2Cl_2 on TiO_2 in O_2. Does the CO product contain the O atom from O_2? If no, that means the presence of O_2 is just to assist the CH_2Cl_2 photodecomposition involving the lattice oxygen. If yes, it is interesting to compare the rate of CO formation related to lattice oxygen and O_2. To answer the question, we have investigated the CH_2Cl_2 photodecomposition in the presence of isotope-labeled oxygen, $^{18}O_2$. Figure 7 shows the IR spectra taken after the indicated times during UV irradiation of $CH_2Cl_{2(a)}$ in the presence of $^{18}O_2$. Just as in the case in $^{16}O_2$, $CH_2Cl_{2(a)}$ is completely consumed by 80 min. The $C^{16}O_{(a)}$ band at 2127 cm^{-1} resulting from lattice oxygen participation is also observed for the reaction in $^{18}O_2$, but a new band appears at 2077 cm^{-1} next to the 2127 cm^{-1} of adsorbed $C^{16}O$. The frequency difference of these two bands is 50 cm^{-1}, which is

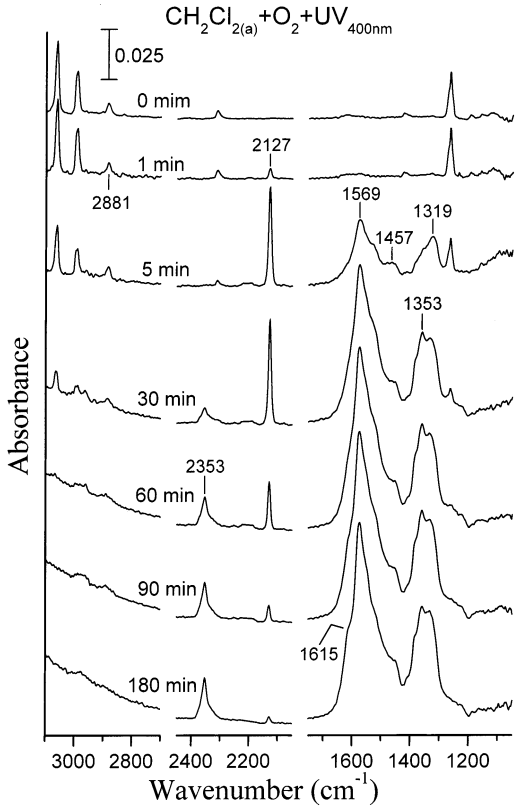

Figure 5. Infrared spectra taken after the indicated times during photoirradation of a TiO_2 surface covered with CH_2Cl_2 in 10 Torr of $^{16}O_2$. The surface was prepared by exposing a TiO_2 surface to 2 Torr of CH_2Cl_2 followed by evacuation at 35 °C. All of the spectra were measured with 5 scans.

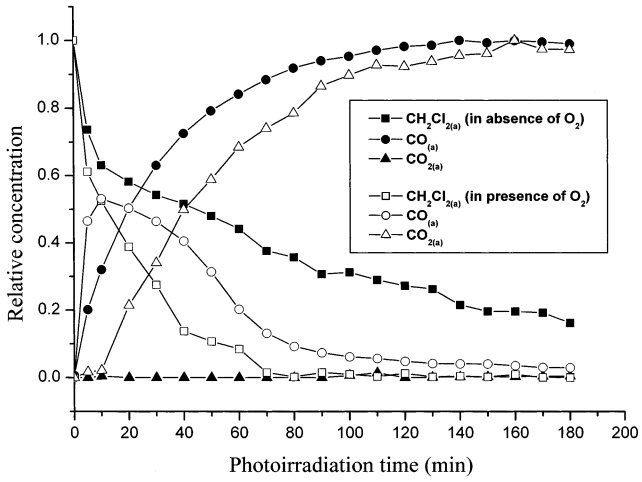

Figure 6. Relative concentrations of CH_2Cl_2, CO, and CO_2 as a function of TiO_2 irradiation time for adsorbed CH_2Cl_2 in the absence and presence of O_2. The CH_2Cl_2-adsorbed TiO_2 surface was prepared by exposing a clean TiO_2 surface to 2 Torr of CH_2Cl_2 followed by evacuation at 35 °C. The maximum amounts of CH_2Cl_2, CO, and CO_2 are scaled to 1.

about the same as that between $C^{16}O$(2143 cm^{-1}) and $C^{18}O$(2091 cm^{-1}) in the gas phase. Therefore the 2077 cm^{-1} is attributed to adsorbed $C^{18}O$. This reveals that $^{18}O_2$ takes part in the formation of carbon monoxide in the $CH_2Cl_{2(a)}$ photocomposition in addition to the pathway of contribution of TiO_2 lattice oxygen. As shown in Figure 7, $C^{16}O_{(a)}$ and $C^{18}O_{(a)}$ are quickly generated upon irradiation of TiO_2. Before ~5 min, the integrated area of 2127 cm^{-1} is about twice of that of 2077 cm^{-1}. However this ratio decreases and becomes about 1 at 30 min. This phenomenon indicates that the process involving lattice oxygen for $CO_{(a)}$ formation is faster in the initial stage, assuming $C^{16}O_{(a)}$ and $C^{18}O_{(a)}$ have the same infrared extinction coefficients.

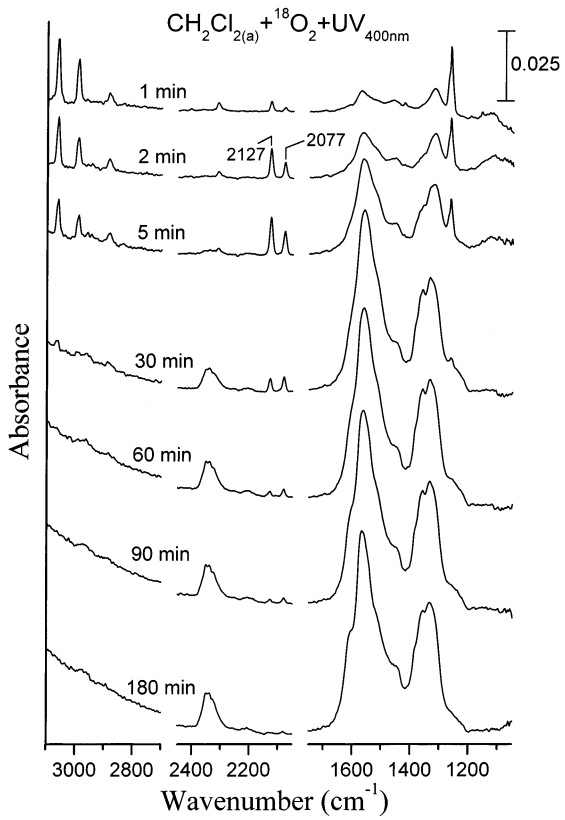

Figure 7. Infrared spectra taken after the indicated times during photoirradation of a TiO_2 surface covered with CH_2Cl_2 in 10 Torr of $^{18}O_2$. The surface was prepared by exposing a TiO_2 surface to 2 Torr of CH_2Cl_2 followed by evacuation at 35 °C. All of the spectra were measured with 5 scans.

In photoillumination of TiO_2 in the absence of O_2, adsorbed CH_2Cl_2 is transformed into $CO_{(a)}$, $CO_{3(a)}$, and $HCOO_{(a)}$. It is certain that the photooxidation of adsorbed CH_2Cl_2 is mediated by TiO_2, because our separate experiments have shown that gaseous CH_2Cl_2 is not subject to decomposition under UV irradiation with the same wavelength. Upon photoirradiation of a semiconductor, excitation of the valence band electrons to the conduction band to form electron−hole pairs is a well-established photoprocess. Following this 10^{-15} s event, the charge carriers may recombine, be trapped, or react with adsorbates. It is believed that there are several possible initiation species for TiO_2-catalyzed photooxidation, including hole, OH•, and oxygen anions.[26−28] If the CH_2Cl_2 photodecomposition on TiO_2 is initiated by hole, in the framework of the band structure model, the occupied orbital levels of adsorbed CH_2Cl_2 should be higher than or matched to the hole levels in order to transfer the electrons from the CH_2Cl_2 to the TiO_2 valence band to initiate the oxidation process. Determination of energy levels can be studied by UV photoelectron spectroscopy. Table 2 compares the previously reported electron binding energies of a few highest occupied orbitals for OH, NH_3, H_2O, CH_3COOH, and C_6H_5COOH on the surface of single-crystal TiO_2 or ZnO. It is found that, for these species, even the highest occupied molecular orbitals are a few electronvolts lower than the valence band edge of TiO_2 or ZnO. Although, no energy level data for adsorbed CH_2Cl_2 on TiO_2 are available in the literature of ultraviolet photoelectron spectroscopy, it is expected that the

TABLE 2: Comparison of Binding Energies of Several Highest Occupied Orbitals of OH, NH_3, H_2O, CH_3COOH, and C_6H_5COOH on ZnO or TiO_2[a]

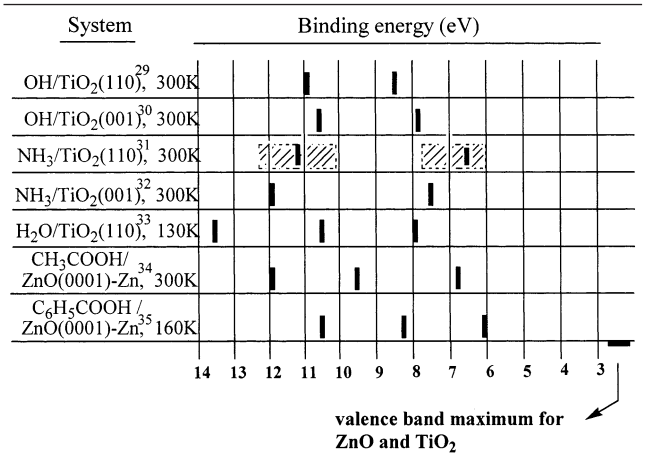

[a] Note that the energy levels are referred to the Fermi level.

HOMO of adsorbed CH_2Cl_2 on TiO_2(001) or TiO_2(110) are also several electronvolts lower than the TiO_2 valence band edge because the ionization potentials of the occupied highest orbitals for CH_2Cl_2(11.3 eV), NH_3(10.2 eV), H_2O(12.6 eV), and CH_3COOH(10.9 eV) in the gas phase are comparable.[36] Unless the occupied orbitals of CH_2Cl_2 on powdered TiO_2 used in this study are shifted a few electronvolts upward, the mismatch between the occupied CH_2Cl_2 orbitals and the TiO_2 hole levels restricts direct electron transfer from CH_2Cl_2 to the electron vacancy at the valence band edge of TiO_2. Although the exact species for initiation of CH_2Cl_2 photodissociation is not clear, it may be due to surface-bound, active oxygen species associated with hole-trapping by lattice oxygen or surface OH. In the CH_2Cl_2 photodecomposition in aqueous solution without O_2 investigated by Catza et al.,[3] they observed formation of HCOOH, CH_2O, and CH_3OH as intermediates and proposed radical mechanisms involving HCO•, $HOCH_2$•, and $ClCH_2$•.

In the presence of O_2, photodecomposition of adsorbed CH_2Cl_2 is accelerated. In addition to the original products of $CO_{(a)}$, $CO_{3(a)}$, and $HCOO_{(a)}$ observed in the case without O_2, CO_2 and H_2O are generated. Previously we have studied the photooxidation of $HCOO_{(a)}$ on TiO_2 and found the formation of CO_2, without CO. So the formation of CO from $CH_2Cl_{2(a)}$ photodecomposition is not via $HCOO_{(a)}$. As $^{18}O_2$ is used in $CH_2Cl_{2(a)}$ photodecomposition, it is found that both $C^{16}O_{(a)}$ and $C^{18}O_{(a)}$ are formed and the amount of $C^{16}O_{(a)}$ is about twice that of $C^{18}O_{(a)}$ in the early stage of photoirradiation, assuming both $C^{16}O_{(a)}$ and $C^{18}O_{(a)}$ have the same absorption coefficient. This demonstrates that photodecomposition of $CH_2Cl_{2(a)}$ to form carbon monoxide in the presence of O_2 is at least via two pathways: one is related to the lattice oxygen just as in the case without O_2 and the other involves adsorbed O_2. Photoirradiation of TiO_2 in O_2 produces active oxygen anion species such as O_2^-, O_3^-, and O_3^{-3} in which only O_2^- survives at room temperature by ESR study.[37] CH_2Cl_2 is not inert to O_2^-. Stoichiometries and kinetics for the reaction of O_2^- with CH_2Cl_2 in dimethylformamide have been reported, with the overall reaction of $CH_2Cl_2 + 2O_2^- \rightarrow CH_2O + 2Cl^- + {}^3/_2O_2$ at 25 °C.[38] Since the TiO_2 surface used in this study possesses OH groups, the possibility of involvement of OH• in the photodecomposition of CH_2Cl_2 cannot be ruled out. There is convincing evidence in the literature supporting OH• radicals as initiating oxidants for photoreactions on TiO_2 surface.[1,39] The mechanism of photoreactions of CH_2Cl_2 on TiO_2 is under discussion.

SCHEME 3

$$CH_2Cl_{2(a)} \xrightarrow{h\nu} CO_{(a)} + CO_{3(a)} + HCOO_{(a)}$$

$$CH_2Cl_{2(a)} + O_2 \xrightarrow{h\nu} CO_{(a)} + CO_{3(a)} + HCOO_{(a)} + CO_{2(a)} + H_2O_{(a)}$$

Conclusion

As TiO_2 is exposed to CH_2Cl_2 at 35 °C, CH_2Cl_2 is adsorbed molecularly and dissociatively to form $CClH_2O_{(a)}$, which decomposes to generate $HCOO_{(a)}$ and $CH_3O_{(a)}$, probably via $-OCH_2O-$ at elevated temperatures above ~100 °C. CO, CO_2, HCl, and CH_2O are detected at higher temperatures. Scheme 3 summarizes the photodecomposition results of CH_2Cl_2 on TiO_2, only showing the photoproducts detected. Since the branching ratios of the photoproducts are not known, the chemical equations in Scheme 3 are not stoichiometrically balanced. The fate of chlorine in the photodecomposition of CH_2Cl_2 is not clear, it is likely remained on the surface. The presence of O_2 accelerates the photodecomposition of $CH_2Cl_{2(a)}$.

Acknowledgment. We thank the National Science Council of the Republic of China for the financial support (NSC 90-2113-M-006).

References and Notes

(1) Fox, M. A.; Dulay, M. T. *Chem. Rev.* **1993**, *93*, 341.
(2) Calza, P.; Minero, C.; Pelizzetti, E. *J. Chem. Soc., Faraday Trans.* **1997**, *93*, 3756.
(3) Calza, P.; Minero, C.; Pelizzetti, E. *Environ. Sci. Technol.* **1997**, *31*, 2198.
(4) Lichtin, N. N.; Avudaitai, M. *Environ. Sci. Technol.* **1996**, *30*, 2014.
(5) Hsiao, C.-Y.; Lee, C.-L.; Ollis, D. F. *J. Catal.* **1983**, *82*, 418.
(6) Basu, P.; Ballinger, T. H.; Yates, J. T., Jr. *Rev. Sci. Instrum.* **1998**, *59*, 1321.
(7) Wong, J. C. S.; Linsebigler, A.; Lu, G.; Fan, J.; Yates, J. T., Jr. *J. Phys. Chem.* **1995**, *99*, 335.
(8) Russell, B. R.; Edwards, L. O.; Raymonda, J. W. *J. Am. Chem. Soc.* **1973**, *95*, 2129.
(9) Mckean, D. C.; Torto, I.; Morrisson, A. R. *J. Mol. Struct.* **1983**, *99*, 119.
(10) Solymosi; F.; Raskó, J. *J. Catal.* **1995**, *155*, 74.
(11) Chuang, C.-C.; Wu, W.-C.; Huang, M.-C.; Huang, I.-C.; Lin, J.-L. *J. Catal.* **1999**, *185*, 423.
(12) Wu, W.-C.; Chuang, C.-C.; Lin, J.-L. *J. Phys. Chem. B* **2000**, *104*, 8719.
(13) Su, C.; Yeh, J.-C.; Chen, C.-C.; Lin, J.-C.; Lin, J.-L. *J. Catal.* **2000**, *194*, 45.
(14) Busca, G.; Lamotte, J.; Lavalley, J.-C.; Lorenzelli, V. *J. Am. Chem. Soc.* **1987**, 109, 5197.
(15) *The Aldrich Library of FT-IR Spectra*, lst ed.; Aldrich Chemical Co., Inc.: Milwaukee, WI, 1985.
(16) Guglielminotti, E. *Langmuir* **1990**, *6*, 1455.
(17) Nakamoto, K.; *Infrared and Raman Spectra of Inorganic and Coordination Compounds*, 4th ed.; Wiley: New York, 1986.
(18) Bianchi, D.; Chafik, T.; Khalfallah, M.; Teichner, S. J. *Appl. Catal. A: General* **1994**, *112*, 219.
(19) Kondo, J.; Abe, H.; Sakata, Y.; Maruya, K.; Domen, K.; Onishi, T. *J. Chem. Soc. Faraday Trans. 1* **1988**, *84*, 511.
(20) Hertl, W. *Langmuir* **1989**, *5*, 96.
(21) Bianchi, D.; Chafik, T.; Khalfallah, M.; Teichner, S. J. *Appl. Catal. A: General* **1995**, *123*, 89.
(22) Fisher, I. A.; Bell, A. T. *J. Catal.* **1997**, *172*, 222.
(23) Bianchi, D.; Chafik, T.; Khalfallah, M.; Teichner, S. J. *Appl. Catal. A: General* **1994**, *112*, 57.
(24) Morterra, C.; Orio, L. *Mater. Chem. Phys.* **1990**, *24*, 247.
(25) Liao, L.-F.; Wu, W.-C.; Chen, C.-Y.: Lin, J.-L. *J. Phys. Chem. B* **2001**, *105*, 7678.
(26) Chuang, C.-C.; Chen, C.-C.; Lin, J.-L. *J. Phys. Chem. B* **1999**, *103*, 2439.
(27) Micic, O. I.; Zhang, Y.; Cromack, K. R.; Trifunac, A. D.; Thurnauer, M. C. *J. Phys. Chem.* **1993**, *97*, 13284.

(28) El-Maazawi, M.; Finken, A. N.; Nair, A. B.; Grassian, V. H. *J. Catal*. **2000**, *191*, 138.
(29) Kurtz, R.; Stockbauer, R.; Madey, T. E.; Román, E. L.; de Segovia, J. L. *Surf. Sci.* **1989**, *218*, 178.
(30) Bustillo, F. J.; Román, E. L.; de Segovia, J. L. *Vacuum* **1989**, *39*, 659.
(31) Román, E. L.; de Sagovia, J. L.; Kurtz, R. L.; Stockbauer, R.; Madey, T. E. *Surf. Sci.* **1992**, *273*, 40.
(32) Román, E. L.; de Segovia, J. L. *Surf. Sci.* **1991**, *251/252*, 742.
(33) Muryn, C. A.; Hardman, P. J.; Crouch, J. J.; Raiker, G. N.; Thornton, G.; Law, D. S.-L. *Surf. Sci.* **1991**, *251/252*, 747.
(34) Vohs, J. M.; Barteau, M. A. *Surf. Sci.* **1988**, *201*, 481.
(35) Vohs, J. M.; Barteau, M. A. *J. Phys. Chem.* **1989**, *93*, 8343.
(36) Turner, D. W.; Baker, C.; Baker A. D.; Brundle, C. R. *Molecular Photoelectron Spectroscopy*; John Wiley & Sons Ltd.: New York, 1970.
(37) Meriaudeau, P.; Vedrine, J. C. *J. Chem. Soc., Faraday Trans 2* **1976**, *72*, 472.
(38) Roberts, J. L., Jr.; Sawyer, D. T. *J. Am. Chem. Soc.* **1981**, *103*, 712.
(39) Hoffmann, M. R.; Martin, S. T.; Choi, W.; Bahnemann, D. W. *Chem. Rev.* **1995**, *95*, 69.